PCCP

Dynamic Article Links ►

Cite this: DOI: 10.1039/c0xx00000x

www.rsc.org/xxxxxx

ARTICLE TYPE

Electronic Supplementary Information

State-to-state resolved differential cross sections for rotationally inelastic scattering of ND_3 with He.

Ondřej Tkáč,[a] Ashim Kumar Saha,[b] Jolijn Onvlee,[b] Chung-Hsin Yang,[b] Gautam Sarma,[b] Chandan Kumar Bishwakarma,[b] Sebastiaan Y.T. van de Meerakker,[b] Ad van der Avoird,*[b] David H. Parker*[b], and Andrew J. Orr-Ewing*[a]

Received (in XXX, XXX) Xth XXXXXXXXX 20XX, Accepted Xth XXXXXXXXX 20XX
DOI: 10.1039/b000000x

Effect of collision energy on the measured DCSs

Small changes to the collision energy could be made by seeding the ND_3 in carrier gases other than Ar. Here, we examine the effects of seeding in Kr and in Xe.

A. ND_3 (in Kr) + He scattering

By seeding the ND_3 in Kr, the collision energy was reduced to 410 ± 40 cm^{-1}, and the velocity map images obtained are shown in Figure S1. The DCSs derived from the experimental data are compared to QM scattering calculations in Figure S2.

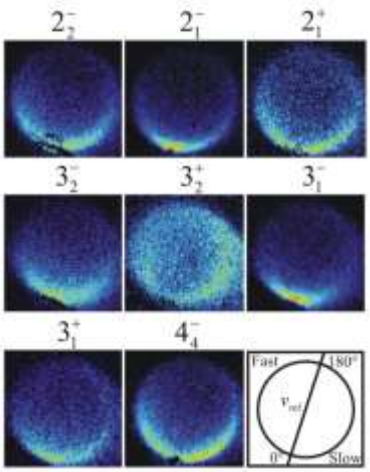

Fig. S1 Experimental velocity map images for inelastic scattering of ND_3 prepared in an initial state $j_k^{\pm} = 1_1^-$ and seeded in Kr. The ND_3 undergoes collision with He at an energy of 410 ± 40 cm^{-1}. Images are labelled by the final rotational level and symmetry of the detected ND_3.

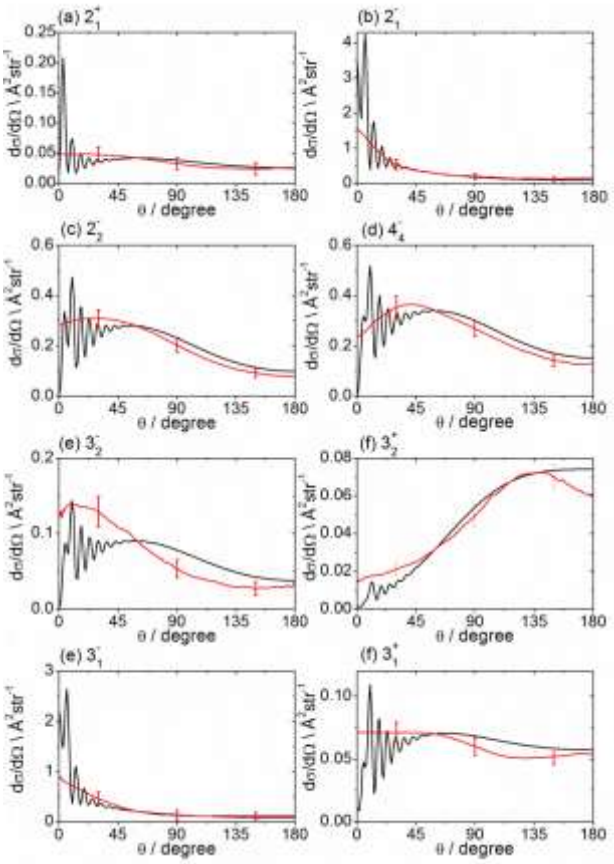

Fig. S2 DCSs for inelastic scattering of ND_3 $j_k^{\pm} = 1_1^-$ (seeded in Kr) with He into various final $j'_{k'}$ and +/– symmetry levels. Red lines are experimental data derived from the raw images in figure S1 following density-to-flux transformation. Black lines are the results of QM scattering calculations. The mean collision energy was 410 ± 40 cm^{-1}.

B. ND_3 (in Xe) + He scattering

By seeding the ND_3 in Xe, the collision energy was further reduced to 400 ± 40 cm^{-1}. Resultant velocity map images are shown in Figure S3, with DCSs derived from the experimental data plotted in Figure S4, where they are also compared to scattering calculation results.

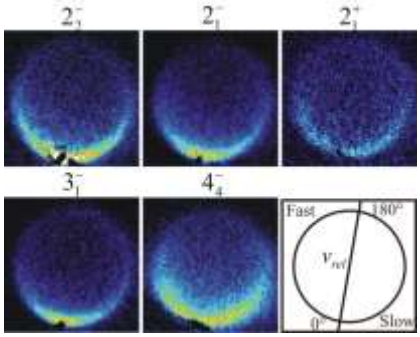

Fig. S3 Experimental velocity map images for inelastic scattering of ND_3 prepared in an initial state $j_k^{\pm} = 1_1^-$ and seeded in Xe. The ND_3 undergoes collision with He at an energy of 400 ± 40 cm^{-1}. Images are labelled by the final rotational level and symmetry of the detected ND_3.

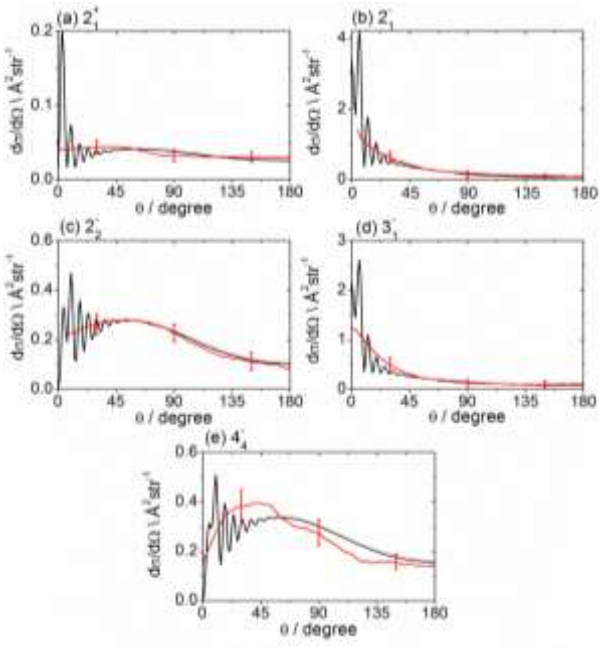

Fig. S4 DCSs for inelastic scattering of ND_3 $j_k^{\pm} = 1_1^-$ (seeded in Xe) with He into various final $j'_{k'}$ and +/– symmetry levels. Red lines are experimental data derived from the raw images in figure S3 following density-to-flux transformation. Black lines are the results of QM scattering calculations. The mean collision energy was 400 ± 40 cm^{-1}.

C. Comparison of computed DCSs at collision energies of 410 and 430 cm^{-1}

Figure S5 compares calculated DCSs for several selected final states of ND_3 produced from the 1_1^- initial state following collisions with He at collision energies of 410 and 430 cm^{-1}. From this comparison, it is evident that most of the DCSs do not change significantly when the collision energy changes by 20 cm^{-1}. Rotational rainbows and diffraction oscillations are clearly visible.

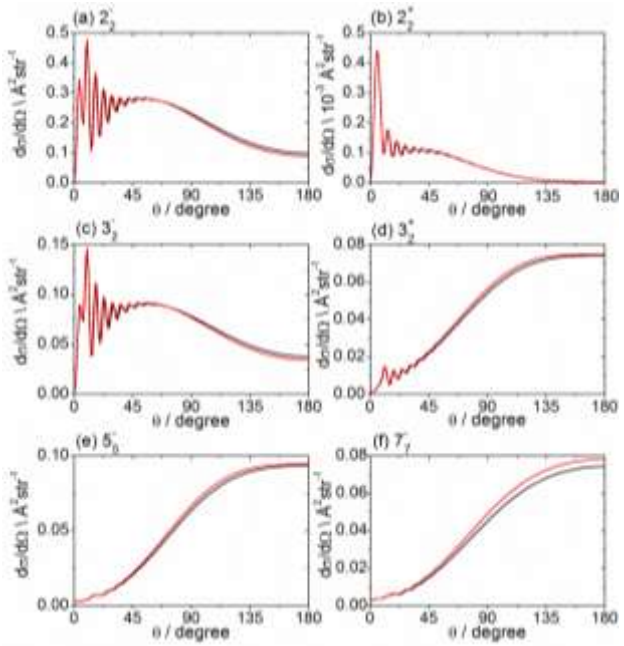

Fig. S5 Calculated He + ND_3 inelastic DCSs for $1_1^- \rightarrow j'^{\pm}_{k'}$ transitions indicated in each panel at collision energies of 410 cm^{-1} (black lines) and 430 cm^{-1} (red lines).

D. Density-to-flux transformation

Figures S6 and S7 show raw DCSs extracted from an uncorrected image measured for inelastic scattering of ND_3 with He into the final level $j'^{\pm}_{k'} = 3_0^-$without hexapole state selection and for the final level $j'^{\pm}_{k'} = 2_1^-$ with the hexapole employed. These DCSs are divided by the angular distribution of the instrument function,as simulated by the Monte Carlo program, which is also shown, resulting in the corrected (symmetric) DCS plotted.

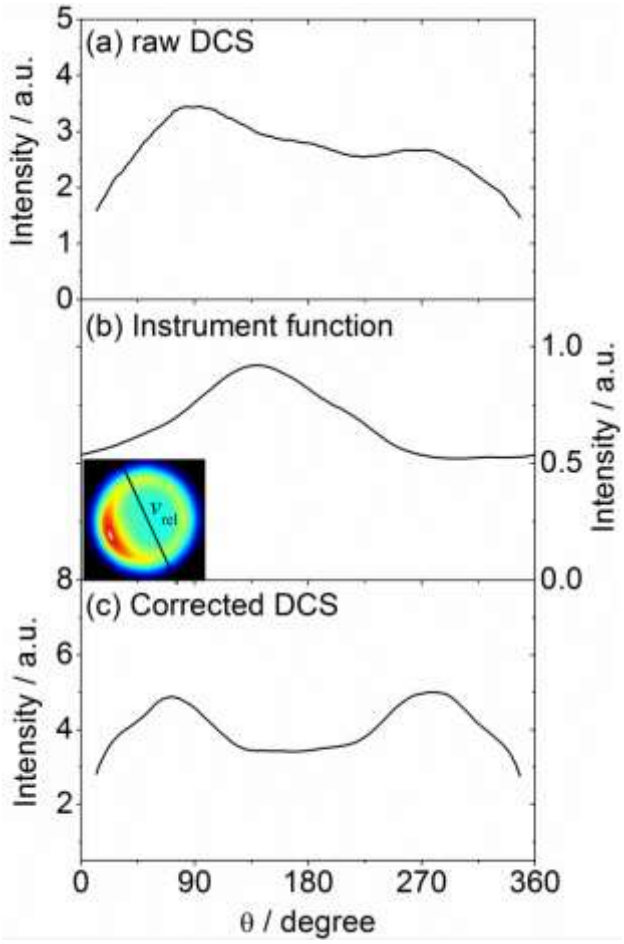

Fig. S6 Raw DCS extracted from an uncorrected image measured for inelastic scattering of ND_3 with He into the final level $j'^{\pm}_{k'} = 3_0^-$ without initial hexapole state selection. (b) Angular distribution of the instrument function simulated by the Monte Carlo program. (c) Corrected (symmetric) DCS acquired by division of the raw DCS by the angular distribution of the instrument function.

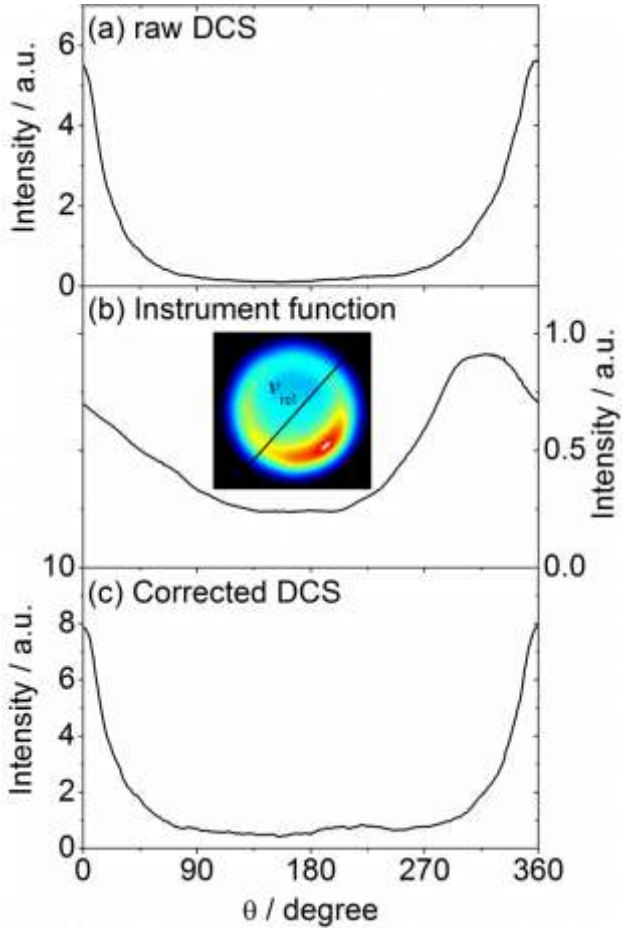

Fig. S7 Raw DCS extracted from an uncorrected image measured for inelastic scattering of ND_3 with He into the final level $j'^{\pm}_{k'} = 2_1^-$ with initial hexapole state selection. (b) Angular distribution of the instrument function simulated by the Monte Carlo program. (c) Corrected (symmetric) DCS acquired by division of the raw DCS by the angular distribution of the instrument function.

Notes and references

[a] *School of Chemistry, University of Bristol, Cantock's Close, Bristol BS8 1TS, UK; E-mail: a.orr-ewing@bris.ac.uk*
[b] *Radboud University Nijmegen, Institute for Molecules and Materials, Toernooiveld 1, 6525ED Nijmegen, The Netherlands; E-mail: parker@science.ru.nl, avda@theochem.ru.nl*